We are IntechOpen, the world's leading publisher of Open Access books Built by scientists, for scientists

6,900
Open access books available

186,000
International authors and editors

200M
Downloads

154
Countries delivered to

Our authors are among the

TOP 1%
most cited scientists

12.2%
Contributors from top 500 universities

CLARIVATE ANALYTICS
BOOK CITATION INDEX
INDEXED

WEB OF SCIENCE™

Selection of our books indexed in the Book Citation Index
in Web of Science™ Core Collection (BKCI)

Interested in publishing with us?
Contact book.department@intechopen.com

Conceptual Study of a Thermal Storage Module for Solar Power Plants with Parabolic Trough Concentrators

Valentina A. Salomoni, Carmelo E. Majorana,
Giuseppe M. Giannuzzi, Rosa Di Maggio,
Fabrizio Girardi, Domenico Mele and
Marco Lucentini

Additional information is available at the end of the chapter

http://dx.doi.org/10.5772/54060

1. Introduction

Technologies and methods for thermal energy storage have been well tested in CSP - Concentrated Solar Power – plants [1, 2]. Solar tower plants (e.g. Solar Two, USA) and advanced parabolic trough plants (e.g. Archimede by ENEA, Italy) use molten salts both as heat transfer and thermal storage fluid. Differently, traditional trough plants (e.g. Andasol, Spain) distinguish the fluid through the solar field (synthetic oil) from the one used in the storage system (molten salt). Hence, storage applications have only been proven in liquid state and in large scale plants.

Concrete is the generally preferred "solid" material for its low cost and good thermal conductivity, already tested at the Platform Solar of Almeria (Spain) and by DLR (Germany) revealing an appropriate response to the specific use, among which a structural stability [3, 4].

Thermal storage of sensible heat using concrete is at present a known procedure, but applications are still limited and some variables (e.g. concrete durability, concrete mixing, etc.) are unclear or not appropriately defined. Briefly, limitations of existing solid thermal energy storage systems include: existing systems are conceived for operating in big capacity plants (skilled personnel and technical infrastructure available); concrete mixtures: actual research is focused on thermal performances optimization regardless costs and durability issues; hygro-thermal issues, not well defined, has not been treated and disseminated.

Nowadays, new mixtures are under study but their characterization seems to be not completed.

Some attempts have been tried incorporating components to increase the conductivity of the composite materials as graphite but this solution increases the cost, however no experience exists in concrete. The technology of concrete production can also contribute to the optimisation of the type of concrete for TES (Thermal Energy Storage), as for instance self compacted concrete.

The main technical objectives of the authors' current research include: 1) development of an appropriate concrete mixing, optimizing chemical-physical and durability performances in a temperature range up to 300°C; 2) thermal sizing of the storage module and its integration within a CSP system. Such results will be obtained through various activities, for some part reported in this Chapter:

- verification of the (hydro)-thermo-mechanical response for the storage module, in its start-up and exercise stages;

- realization and experimentation of a prototype at reduced scale;

- conceptual project of a thermal storage module, including a synthesis of both technical and economical aspects.

Among the innovative research and development items, we recall:

a. The system is constituted by modular blocks made by innovative concrete material whose mix design is being investigated [5]. The constitutive characterization of the concrete mixture chosen as thermal storage, once passed theoretical to experimental investigation, will represent a fundamental cognitive relapse in the context of cementitious materials subjected to high temperature [6]. In its basic aspects it will be inspired by complementary applications within an already operative project to which ENEA, and the Universities of Padua, Trento and Rome, Italy, are contributing. The research outcomes have already proved the possibility to satisfy the features and behaviour requested for such an application in terms of thermal and mechanical characteristics. It is anyway necessary to deepen the structural behaviour and aspects regarding durability and possible local small damaged spots which can bring to a possible loss in functionality of the component, being nowadays an open question;

b. The tubes in which the heat-transfer fluid flows are immersed inside the concrete matrix. The up-to-now adopted constructive solution used by DLR consists in a tube bundle with adequately supported pipe fittings and in a particular distribution within concrete casting [3, 4, 7, 8]. A sort of concrete mono-block comes out: the free water contained within its concrete matrix hardly leaks, especially during its first heating phase. This can bring to high pressure gradients, causing complete component damage or reductions in thermal performance.

Our research activity will match a wide application range of expertise in order to avoid original problems of module cracking. A balanced new-type concrete mixture, derived from pre-

vious researches, will be cast under innovative procedures. Piping would derive from heat exchanger applications with specials interface layers also experienced in nuclear plants. Start-up and operational phases would be conceived to limit matrix pressure stress.

2. The SOLTECA Project

The SOLTECA Project contextualizes TES in solid media within the Italian context; the main objectives of the Project include:

- development of an appropriate concrete mixing so to optimize its chemical-physical properties, durability and performance at temperatures between 80-300°C;

- thermal design of a storage module and its integration in CSP systems.

The Project is addressed to solar plants with innovative aspects and characteristics such as: small size plants with a peak power between 0.5-5 MWe, to be more easily placed in the territory; sensible heat storage in concrete with ad-hoc mixing; modular structure of the storage system with elements of reduced dimensions so to be pre-cast and to limit the efforts during degas phases at start-up; capability of returning energy to the heat-transfer fluid at temperatures between 120-300°C; limitation of the storage specific cost between 20-30 €/ kWh_th; use of a heat-transfer fluid with low environmental impact (possibly water); coupling of the solar plant and the storage system with ORC (Organic Rankine Cycles) groups and biomass plants.

It is to be underlined that the maximum operational temperature for concrete is fixed at about 300°C; if water is chosen as heat-transfer fluid, the maximum temperature will be appropriately reduced to limit the service pressure.

As stated, TES is based on CSP systems and the technology has been developed for power plants (SPP, Solar Power Plants) of big dimensions; most of the solar source power comes from the so-called "sun-belt", i.e. the most irradiated area of the planet such as North Africa and Middle East. Anyway the concentrated solar technology can be adopted even in Southern Europe and Italy by integrating it with other renewable technologies which will have to contribute to the growing European demand for "green electricity".

The thermodynamic solar plants produce energy following the same process as for the conventional vapour plants, but using solar radiation as a primary energetic source in agreement with the scheme of Figure 1 for a sensible heat storage system in solid media where energy charge and discharge occur via a heat-transfer fluid circulating in an embedded piping system.

The prior objective in the design phase of a SPP is the definition of the plant configuration and of the single component dimension so to minimize the cost of the produced energy unit, i.e. the Levelized Energy Cost (LEC).
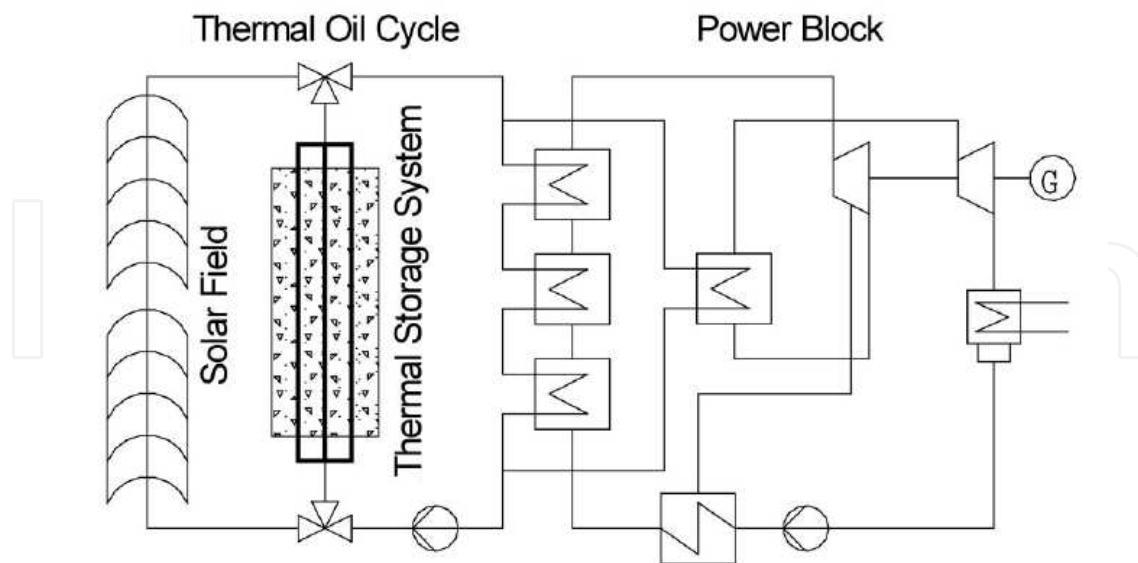
Figure 1. General scheme of a thermodynamic solar plant [8].

3. Storage issues for renewable energies

One of the major restraint to the development of energetic systems from renewable sources is given by the uncertainty with which these sources give energy to the plant. Hence the availability of storage systems is a key-factor in both development and success of a technology for the production of heat or electric energy by using solar radiation for the daily and the long-term use. Nowadays systems able to store high quantities of energy with reduced costs and sizes compatible to those of the serviced plants are not defined yet; the basic principle according to which a storage energy system is used is that of trying to align the generation curve of these plants with the one coming from the users requirements. Whereas the former is linked to the -seasonal or daily- variation of solar energy, the latter depends on the users type to be served (industrial, domestic or services) so that there is no connection between the two.

In general, the main functions performed by a storage system within a SPP are:

a.   buffering during variable sunshine periods,

b.   time shifting in using available radiation,

c.   increment in the annual Capacity Factor and consequent reduction in the cost of produced energy,

d.   more regular production of energy.

Storage allows for facing the oscillatory trend of incoming radiation (Figure 2) and contemporaneously shifts the use of radiation, in excess during the central hours of the

day, towards the late-evening hours. A storage capacity able to allow the plant for operating at its nominal power for 24 hours is theoretically but not practically reachable; following the minimum LEC criterion, the storage and the collectors system sizes must be simultaneously correlated and optimized. As shown in Figure 3, a variety of energy storage types is possible, some already widely used (e.g. in the hydroelectric field), others in development.
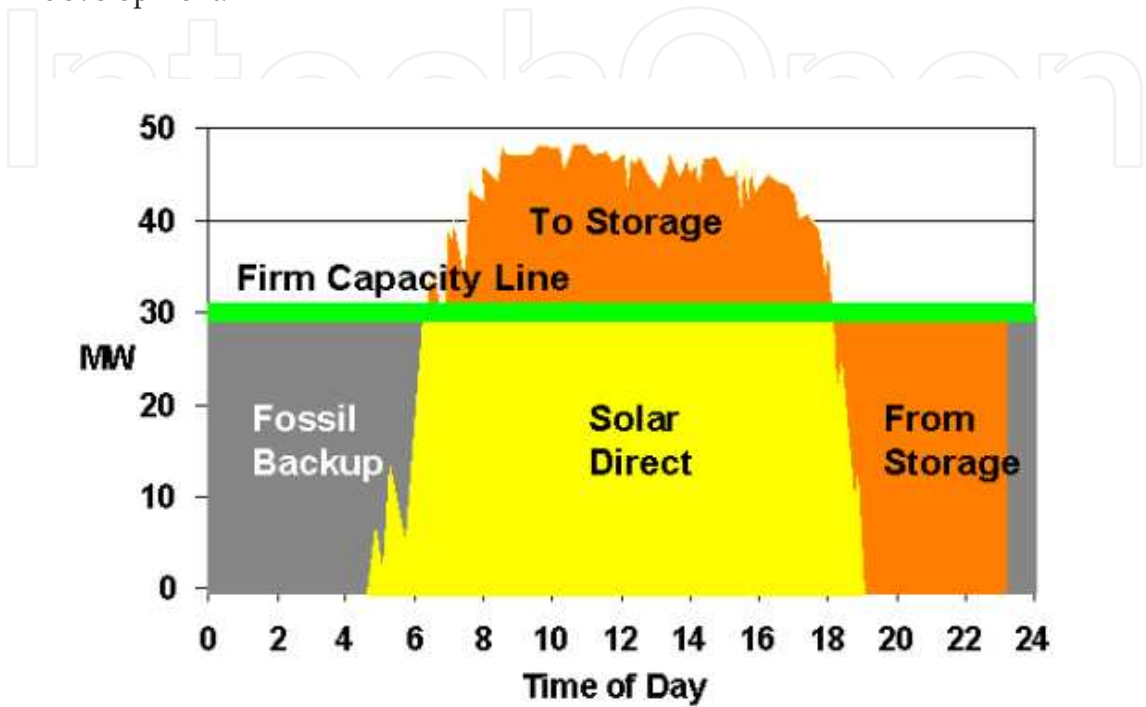
Figure 2. Daily operation for a solar plant with storage system and integration [3].

A complete storage process involves at least three phases: charge, conservation of the stored energy and discharge. In real systems, some of the described steps can occur simultaneously and each of them can even occur more than once for each storage cycle, so that modelling these components becomes a very complicated matter.
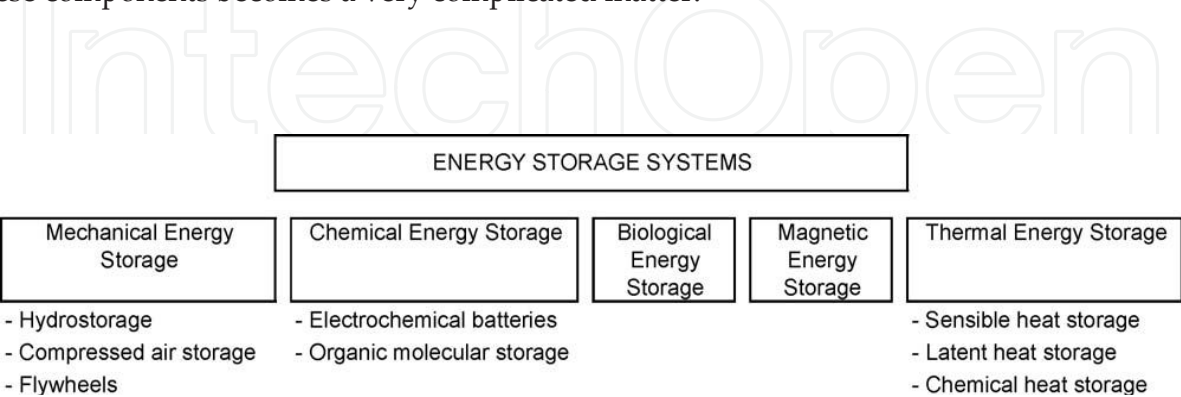
Figure 3. Types of storage system [9].

Multiple aspects must be considered during the design phase for thermal storage systems; from the technical viewpoint, the most relevant specifications are:

• high energy density in the storage medium (storage capacity);

• good heat transfer between Heat Transfer Fluid (HTF) and storage medium (efficiency);

• chemical and mechanical stability of the storage medium (a high number of charge and discharge cycles must be sustained);

• compatibility between HTF and heat exchanger and/or storage material (safety);

• full reversibility of charge/discharge cycles (durability);

• low thermal leakages;

• control easiness.

Moreover, the most important design criteria from the technological point of view are: operational strategies, maximum charge, loss in nominal temperature and specific enthalpy during charge, integration in the power production plant.

3.1. Types of heat storage

Sensible heat storage: thermal energy can be stored via the induced temperature variation in the material, corresponding to an internal energy variation for the sensible heat storage. Among solid materials, e.g. concrete is chosen in the various applications for its low cost, availability and easy workability; additionally, it is a material with high specific heat, good mechanical properties (e.g. compressive strength), thermal expansion coefficient close to the steel one (material used for piping) and high mechanical strength to cyclic thermal loads.

Latent heat storage: thermal energy for some substances can be stored in a nearly-isotherm manner as latent heat linked to phase changes; the materials used for such a technology are named Phase Change Materials (PCM). PCM allow for accumulating high quantity of energy in relatively small volumes, so resulting among the solid media at lowest cost for the various storage concepts.

3.2. Materials for sensible heat storage

The cumulated thermal energy within certain mass of material can be notoriously expressed as

$$Q = \rho \cdot \bar{c}_p \cdot V \cdot \Delta T \tag{1}$$

where it is just to be observed that the specific heat has a mean value within the exercise temperature range.

As previously reported, for being a material usable in a TES-type application, a low cost is needed as well as a good thermal capacity $\rho \bullet \bar{c}_p$. An additional fundamental parameter for

sensible heat TES is the velocity at which heat can be released or extracted; such a character-istic is function of the thermal diffusivity

$$\lambda = \frac{k}{\rho \cdot \overline{c}_p}$$
(2)

in which k is the material thermal conductivity.

Concrete and ceramic materials, both tested at the Platforma Solar de Almeria (PSA), present appropriate characteristics for being adopted as sensible heat storage media.

Table 1 shows the main properties for the most frequent solid storage materials in literature; to improve the "soft" characteristics of an ordinary concrete, a high temperature concrete (HTC) has been studied whose features have been compared to those of a castable ceramic material (Table 2).

Storage medium	Temperature		Average density (kg/m³)	Average heat conductivity (W/m K)	Average heat capacity (kJ/kg K)	Volume specific heat capacity (kWh$_t$/m³)	Media costs per kg (US$/kWh$_t$)	Media costs per kWh$_t$ (US$/kWh$_t$)
	Cold (°C)	Hot (°C)						
Sand-rock-mineral oil	200	300	1700	1.0	1.30	60	0.15	4.2
Reinforced concrete	200	400	2200	1.5	0.85	100	0.05	1.0
NaCl (solid)	200	500	2160	7.0	0.85	150	0.15	1.5
Cast iron	200	400	7200	37.0	0.56	160	1.00	32.0
Cast steel	200	700	7800	40.0	0.60	450	5.00	60.0
Silica fire bricks	200	700	1820	1.5	1.00	150	1.00	7.0
Magnesia fire bricks	200	1200	3000	5.0	1.15	600	2.00	6.0

Table 1. Properties of solid storage media [9].

Material	Castable ceramic	High temperature concrete
Density [kg/m³]	3500	2750
Specific heat at 350 °C [J/kg K]	866	916
Thermal conductivity at 350 °C [W/m K]	1.35	1.0
Coefficient of thermal expansion at 350 °C [10⁻⁶/K]	11.8	9.3

Table 2. Comparison between castable ceramic and HTC

4. Concrete storage

The German Aerospace Centre (DLR) within the Project "Midterm Storage Concepts—Fur-ther Development of Solid Media Storage Systems" developed from 2001 to 2003 has al-ready started the development of sensible heat storage-based technology in solid media. The main points of the Project were the development of an efficient material for heat storage and the technology experimentation with a test unit with the size of 350 kWh [3, 4, 7, 8].

Hence such a technology is known and studied but it is not contextualized to other scenarios, as well as uncertainties exist in term of concrete mixing and durability.

Solid storage systems adopting concrete fall in the category of passive storage systems which are generally "double-material": HTF flows in the storage just to charge and discharge a solid material. HTF transfers the heat received from the source of primary energy (the sun) towards the storage module during the charge process and receives energy from the module itself during discharge according to the scheme of Figure 4; such system are even named *regenerators*. The principal disadvantage of regenerators is that the fluid temperature decreases during discharge as the storage medium chills. An additional problem is that heat transfer is relatively low.

The storage medium contains a piping exchanger for the heat transfer from HTF to the storage and *viceversa*, as depicted in Figure 4. Such a heat exchanger represents a significant part of the costs for the whole investment of the plant. The definition of the geometric parameters, as diameter and number of pipes, is also fundamental for the final result from the performance viewpoint.
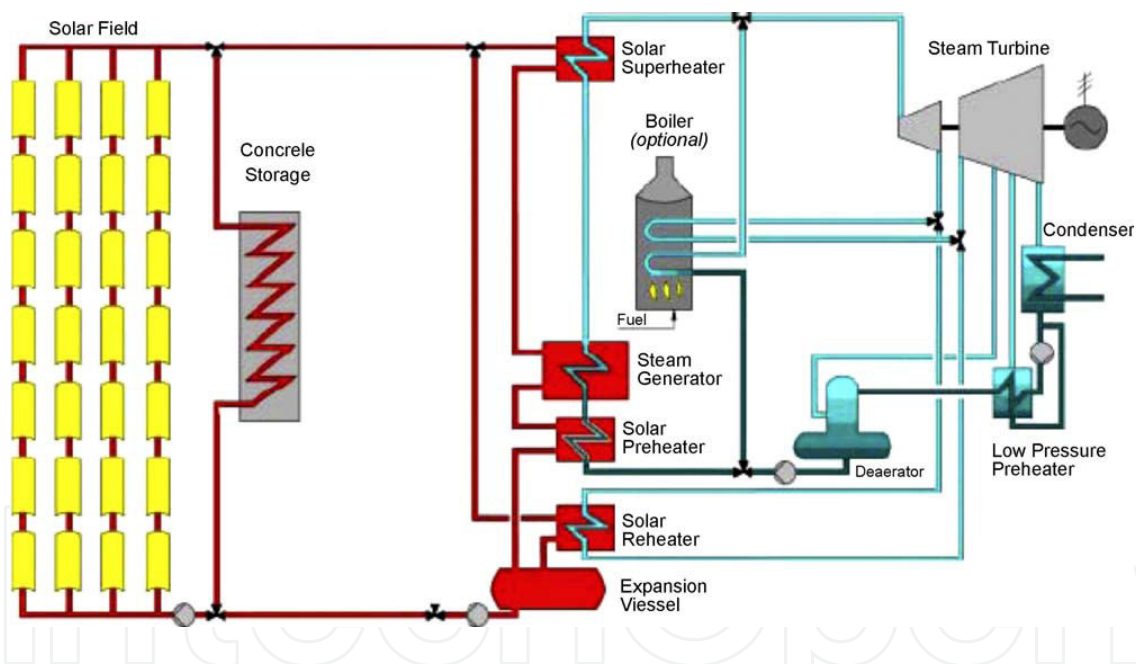

Figure 4. Integration scheme of an indirect storage through solid medium [3, 9].

The advantages of concrete storage systems are:

- low costs of storage media,

- high thermal exchange fluxes within the solid (or from this one towards outside) due to the contact between piping and concrete,

- easy workability of the material,

- low degradation of heat transfer between exchanger and storage medium.

Among the main disadvantages:

- costs increment for exchanger and engineering in general,

- long term instability,

- effective reachable charge level.

With reference to Figure 5, temperature profiles of the material are reported along the channel axis; it is to be noticed that areas underlying the curves are proportional to the quantity of energy if we refer to Equation (1). According to this expression the component's storable energy is proportional to the existing ΔT between the condition of complete charge and discharge. If all the material were first heated and successively uniformly cooled, its storage capacity would be proportional to the area limited by the two horizontal dashed lines. Considering that, in real transients within material, thermal fields develop with the shown qualitatively profiles, a reduced capacity of the system comes out, i.e. there are zones of material which do not contribute to the process (thermally inactive). Hence the objective of the design is to reduce these zones and the parameters on which it is possible to intervene are material itself (via the diffusivity) and geometry (distance between pipes and exchange coefficient).
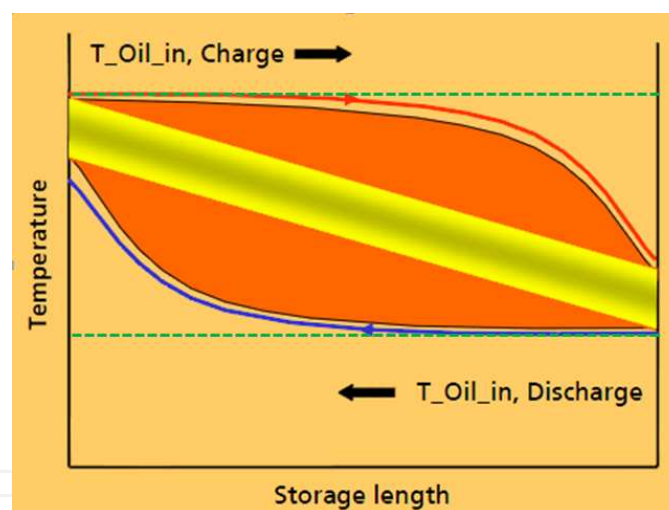

Figure 5. Storable energy within the solid [8].

5. Pre-design procedure

5.1. Definition of storage operational conditions

As stated, even if concrete TES systems have been already studied, they appear to be still in a development phase, so that preliminary analyses are necessary to define design procedures and guidelines for future upgrades.

A simplified approach is here proposed for modelling concrete based on a continuum material model with constant parameters. Considering the characteristics of the plant, an initial design of the different components is performed so to define the operational storage conditions.

With reference to a fixed design plant point, i.e. by assuming in input an effective radiation value and fixing a Solar Multiple value (ratio between the thermal power delivered by the collectors in the design conditions and the nominal power requested by the user),

$$SM = \left. \frac{P_{solar\_field}}{P_{power\_block}} \right|_{Design\_point} \tag{3}$$

the preliminary analysis leads to the parameters of Table 3.

PLANT CHARACTERISTICS		
Nominal radiation	[W/m^2]	700
Solar multiple		2
Plant thermal power	[kW]	4500
m_{nomTES}	[kg/s]	11.33
$v_{\_fluid}$	[m/s]	1
Heat-transfer fluid		H_2O
Charge time (t_c)	[h]	1
CONCRETE PARAMETERS		
ρ	[kg/m^3]	2666
c_p	[J/kg °C]	800
k	[W/m °C]	2
STORAGE EXTREME TEMPERATURES		
T_{in_charge}	[°C]	175
T_{out_charge}	[°C]	125
$T_{in\_discharge}$	[°C]	80
$T_{out\_discharge}$	[°C]	130
Complete charge level		90% ΔT

Table 3. Design characteristics and parameters.

For the material a conductivity value higher than the real one has been assumed, i.e. 2 W/m °C, so to directly refer to a value of k close to the fixed target one and anyway reachable in a short period.

With reference to the storage extreme temperatures, it comes out:

- maximum T of incoming fluid in the charge phase. This value is restrained by the maximum reachable T outgoing the solar field, so that T_{max_in} = 175 °C is assumed;

- maximum T of outgoing fluid in charge phase. This value is restrained by the maximum sustainable T incoming the solar field. Hence the assumed value is the one for which, at equal ΔT in the collectors line, a mass capacity double to the nominal one is required, so T_{max_out} = 125 °C;

- minimum T of incoming fluid in discharge phase. This value is restrained by the water T outgoing from the exchanger supplying the power block in the working nominal conditions. Hence T_{min_in} = 80 °C;

- minimum T of outgoing fluid in discharge phase. This value is restrained by the minimum required fluid T incoming the exchanger supplying the ORC turbine. The imposed value is subsequently T_{min_out} = 130 °C.

It is to be noticed that the ΔT under which the extreme sections work is the same and it is equal to 45°C (Figure 6); additionally, considering the radiation conditions relative to a reference Italian site and the industrial nature of the typical user, t_c = 1h has been assumed.

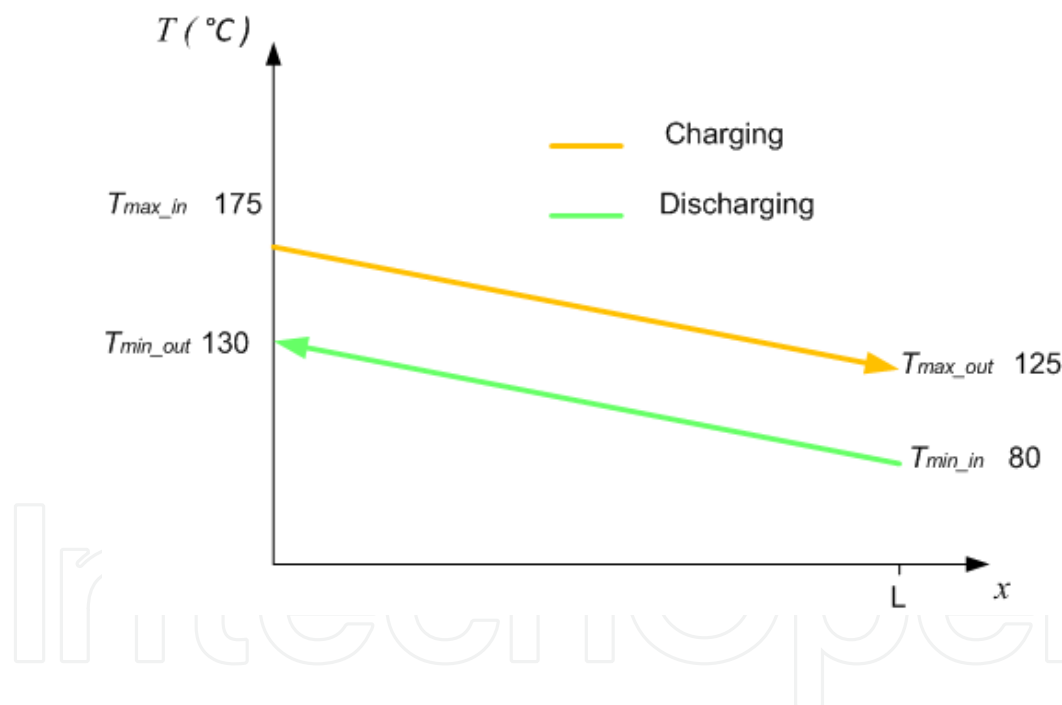**Figure 6.** Restraints to HTF temperatures.

5.2. Definition of the physical model

A storage unit as the one considered here is composed by a piping bundle embedded within concrete for allowing fluid flow through it. The pipes, parallel one to the other, have axes (with reference to Figure 7) at a distance d_a. For the definition of the physical model, the same conditions have been assumed for each parallel channel, so that the storage module is considered to be composed by sub-units, named *elements*, put in parallel [10].
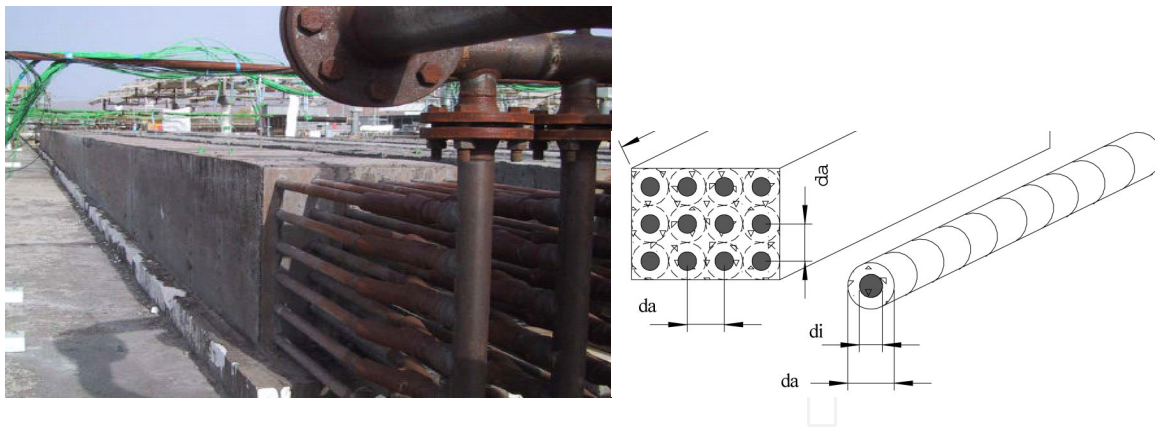
Figure 7. Typical storage module [3].

One element is composed by a concrete drilled cylinder with diameter d_a, in contact with a pipe with internal diameter d_i; the storage medium is characterized by thermal conductivity k, specific capacity per unit mass cp and density ϱ. Even if the storage material inside contiguous cylinders is neglected, such a simplification is necessary for implementing an efficient algorithm.

By having this in mind, the problem of analysing the storage system moves from the study of the module to that of the single channel for which the initial section is the one of the incoming HTF during charge, whereas the final section is the outgoing one during the same phase.

By referring to an initial development stage for an innovative component, an analytical method is searched so that, via the application of a single formula or the implementation of a simple numerical procedure, it allows for reaching general evaluations on the main parameters involved in the design. Such a research stage is additionally adequate, with reference to the medium-term, considering the industrial potential of the Project.

In the following the main features of the procedure are described.

5.3. Analysis of the channel initial section

The initial section, located at the entrance of the hot fluid coming from the solar field, is the one subjected to the highest temperatures so resulting as the most critical one from the viewpoint of the thermo-mechanical design. In fact, by considering the humidity transport and dehydration phenomena effectively taking place in concrete (see e.g. [2, 11]) so that this section will be subjected to the highest thermal flux, it will sustain even the highest internal overpressures with the possibility of being exposed to spalling [12]; such a phenomenon is to be clearly avoided during first heating.

By following [13] with a distribution of piping bundles resembling an equilateral triangle (Figure 8), the attributable zone of each pipe far from the module external border is an hexagon which can be confused with the circumscribed circumference. On this circumference the fluxes can be practically considered as negligible and the entire analysis brought back to a single cylindrical channel with adiabatic external surface.

It is hence fully justified the necessity of a specific analysis for the considered section; in the following dimensionless parameters will be referred to, relative to the section only, as already occurs when studying *pebble bed* storage systems when dimensionless parameters such as porosity or specific exchange surface for unit length are fundamental.

To transfer the procedures adopted for pebble bed systems to embedded piping storage ones, a characteristic "porosity" of the section can be defined, determined by the area crossed by the fluid (not to be confused with the material one) in the following way (Figure 9)
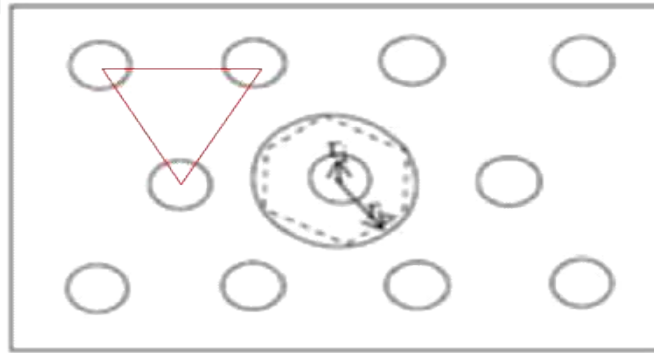
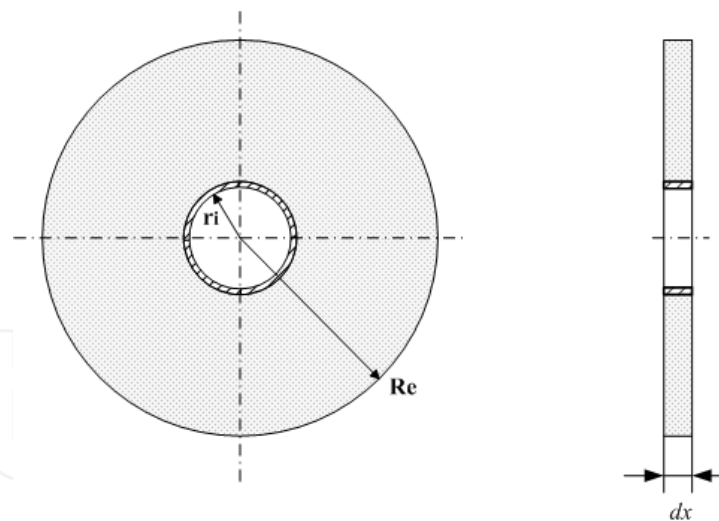**Figure 8.** Location of the piping bundle and elementary cell [13].

Figure 9. Geometrical parameters of the initial section.

$$\varepsilon = \frac{A_f}{A_{tot}} = \frac{\pi R_i^2}{\pi R_e^2} = \left(\frac{R_i}{R_e}\right)^2 \tag{4}$$

Such a porosity is obviously linked to the ratio between phases

$$\varepsilon = \frac{A_f}{A_{tot}} = \frac{A_f}{A_s + A_f} = \frac{1}{\dfrac{A_s}{A_f} + 1} = \frac{1}{\dfrac{1}{f} + 1} = \frac{f}{1 + f} \qquad (5)$$

And the specific exchange surface per unit length is defined

$$A_{sp} = \frac{2\pi R_i}{\pi R_e^2} = \frac{2R_i}{R_e^2} = \frac{2\varepsilon}{R_i} \qquad (6)$$

A first consequence of adopting such an approach is that the storage module length becomes a parameter depending on the assumed section geometry, which is even physically justified by considering that the length is restrained by the production, at the end of the charge phase, of an outgoing flux at temperature not higher than the maximum sustainable one incoming the solar field. With reference to the charge phase it is clear that, for a given charging time, if the initial section does not reach a temperature distribution corresponding to the level assumed as complete charge, the same applies to the final sections so that the simulation of the entire channel is an useless effort.

Going into the specificity of the analysed section, the objective is to be able to estimate the relative *charging time* or, in a dual manner, the temperature level reached in correspondence of the external material circumference in a fixed interval of time. The charging time for a section is defined as the necessary time so that, at the corresponding abscissa, the temperature at the external concrete circumference of pertinence reaches a fixed value T_R^* at which the charge phase can be considered as concluded.

The interval of interest can be represented by the sum of two contributions

$$t_c = t_d + t_s \qquad (7)$$

where t_d is the radial diffusion time necessary for heat to reach the external surface and t_s the rising time necessary for heat flux to increase the temperature T of that surface up to the fixed value.

As regards the former term, in literature the following estimate is proposed [14]

$$t_d \propto \frac{s^2}{\lambda} = \frac{s^2}{C_1 \cdot \lambda} \qquad (8)$$

in which s is the material thickness subjected to heating and C_1 a proportionality coefficient linked to geometry.

The application to the given cylindrical geometry and the comparison with the results coming from the numerical procedure described in the following lead to

$$t_d = \frac{(R_e - r_i)^2}{13 \cdot \lambda} \tag{9}$$

Let's now examine the term related to the rising time; for doing this the following terms are introduced

$$C = \rho \, c_p \cdot \pi (R_e^2 - r_i^2) \, l \tag{10}$$

$$R = \frac{1}{2\pi \, r_i l \, h} + C_3 \frac{\ln\left(R_e/r_i\right)}{2\pi \, l \, k} \tag{11}$$

where C is the capacity term for the considered section, R the thermal resistance term given by the resistance due to the convective exchange on surface and by the solid internal conductivity, l the channel length assumed unitary, $C_3 = 0.72$ an empirical corrective coefficient calibrated from comparison with the results of the Finite Element model.

By observing that the product between the two above terms has the dimension of time,

$$t_1 = R \cdot C \tag{12}$$

and through the electrical analogy with resistive-capacitive circuits, it is immediate to recognize in t_1 a thermal charging time.

Whereas

$$T_R^* = C_2(T_{ing} - T_{ini}) + T_{ini} \tag{13}$$

in which C_2 is the fraction of engine ΔT assumed as sufficient to define the material as charged.

The analytical formula to calculate the charging time is

$$t_c = t_d - R \cdot C \cdot \ln\left(\frac{T_{ing} - T_R^*}{T_{ing} - T_{ini}}\right) \tag{14}$$

Equation (14), despite the presence of empirical calibration coefficients, is an analytical-type relation being derived from an exact physical model and it is pretty original. It is obtained by integrating the Fourier equation in the hypothesis of high Biot's numbers, giving an exponential-type trend for temperature

$$T(t)\big|_{r=R_e} = T_{ing} + (T_{ini} - T_{ing}) \cdot \exp\left[-\frac{t - t_d}{R \cdot C}\right] \tag{15}$$

where at the l.h.s. there is the temperature in correspondence of the external radius of the considered initial section, function of time.

By inverting Eq. (15) so to make time explicit, the above Eq. (14) is obtained.

The comparison between time histories of temperature given by Eq. (15), blue curve, and the numerical procedure, yellow curve, is depicted in Figure 10 with reference to a transient of 1 hour applied to a reference geometry.
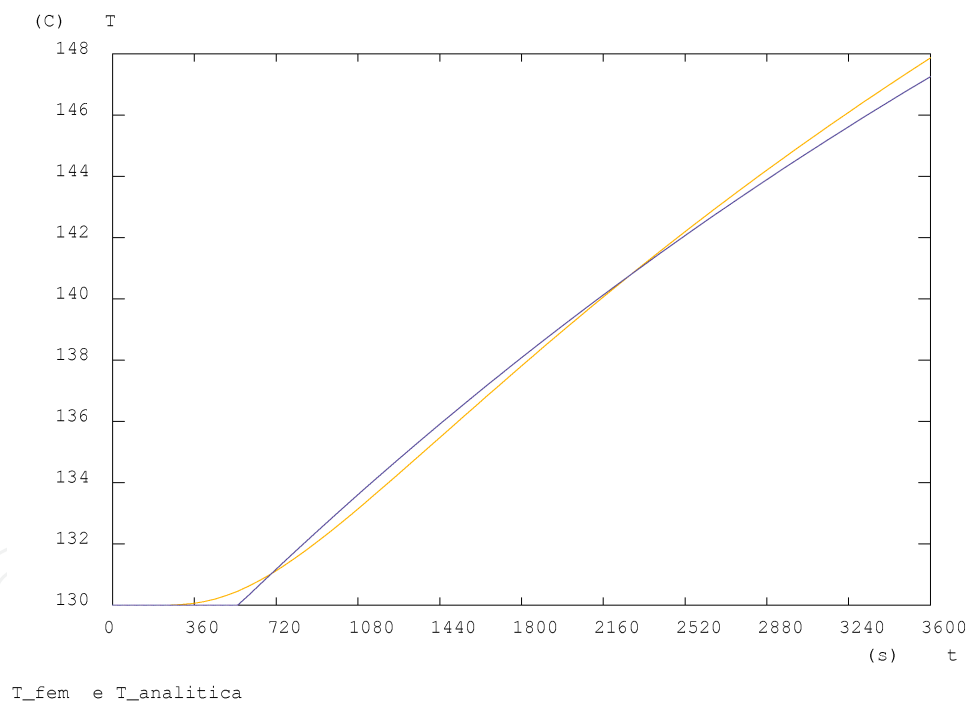

T_fem e T_analitica

Figure 10. Validation of the analytical formula (Eq. (15)).

By varying the geometrical parameters, the difference between curves remains small, so that the obtained analytical formula is assumed to be validated. The formula, once T_R^* is fixed for a section, has the aim of predicting the time necessary to have this level reached, so the comparison must be performed at equal temperature evaluating the horizontal distance between curves, i.e. the difference between rising times from the two procedures to arrive at a given temperature. Additionally the resulting difference is not to be considered as an absolute val-

ue but relatively to the total charging time, that is a difference of 300 s with respect to an imposed charging time of 3600 s is fully acceptable in the initial design phase of the storage.

For sake of brevity the (similar) procedure for analysing the final channel section, as well as the Schumann analytical model (for pebble bed-type systems) [15] applied to this specific context have not been reported in this Chapter.

5.4. Application of the simplified design method

The development of a simplified design methodology for storage systems of the considered type represents a first goal for the developed research.

The starting point is an initial design for the plant; on the basis of these data the following operative scheme is followed.

i.   Channel section geometry. The geometrical parameters of the initial channel section (i.e. piping radius and external material radius) are defined (Figure 11).
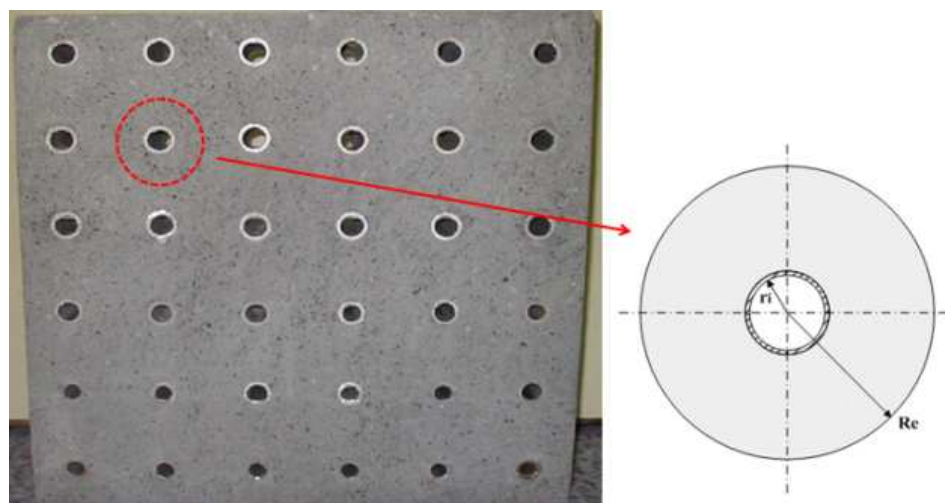

Figure 11. Initial section [3].

ii. Calculation of the number of channels in parallel. Based on the hypothesized piping geometry and on fluid velocity and density, the capacity passing through the channel is defined. Being know the total plant capacity in nominal conditions, by dividing it to the determined unitary capacity, an estimate of the number of channels to be put in parallel is obtained to drain the whole flux.

iii. Initial section analysis. Eq. (15) is applied for calculating the charging time of the initial section for evaluating the reachable entrance charge level.

$$T(t_c)\big|_{r=R_e} = T_{ing} + (T_{ini} - T_{ing}) \cdot \exp\left[-\frac{t_c - t_d}{R \cdot C}\right] = 170°C \qquad (16)$$

If during the imposed charging time it is not possible to charge the section at a fixed temperature, even in the following sections such a level would not be reachable; on the basis of this simple result it is hence necessary to change the assumed geometry and iterate phases II and III.

The fixed completed charge level is instead

$$T^* = 0,9\Delta T = 0,9\left(T_{ing} - T_{ini}\right) = 170,5°C \tag{17}$$

so that the hypothesized geometry allows for a practical complete charge of the initial section.

iv. Channel length definition with graphical method. The section geometry is assumed as input for the Schumann's model.

a) A very long channel is hypothesized, L = 400 m.

Profiles of fluid temperature T_f are drawn along the channel for time instants up to the imposed charging time and an horizontal line is superimposed, relative to the maximum value of T_f at the exit. The point in which the profile relative to $t = t_c$ crosses this line is determined and the corresponding channel length value is read along the abscissa's axis (Figure 12).

The temporal trend of the fluid temperature is drawn on the final section with reference to the length of 300 m (Figure 13) and this value is checked against the maximum one, calculating again the mean value at the final section.
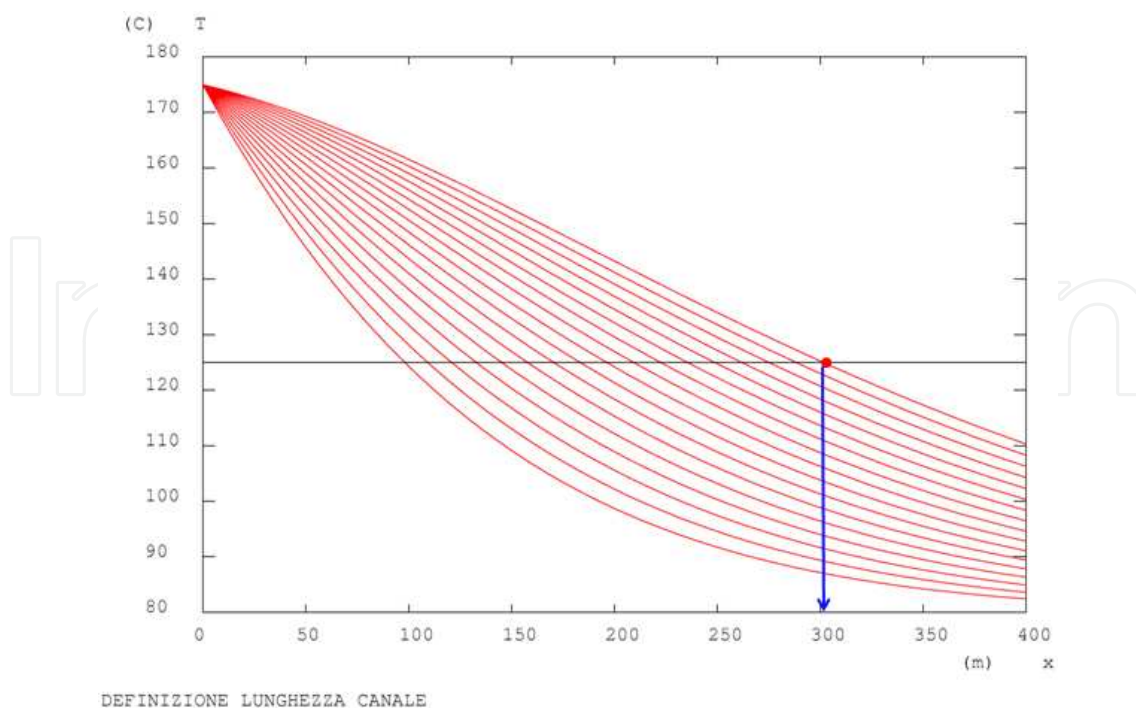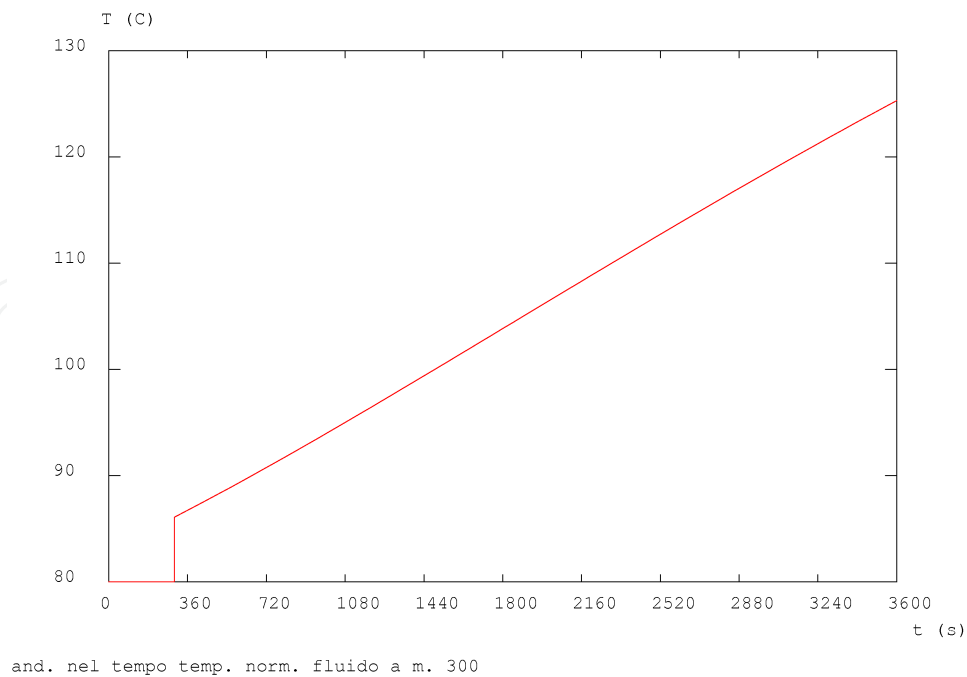

Figure 12. Channel length definition.

and. nel tempo temp. norm. fluido a m. 300

Figure 13. Temperature trend T_f.

v. Final section analysis. The calculated mean value allows for obtaining the tempera-ture at the cold corner at the imposed charging time. Such a temperature is to be verified to correspond to the required charge level. It is to be noticed that in this section the condition of first heating is being evaluated.

vi. Finite Element simulation of the obtained configuration. Only at this stage, after having defined a possible module geometry via analytical formulas and with re-sults in time of the order of about 1 min, a verification via FE models can be con-ducted so to even calculate the effective energy released to the material.

6. Numerical modelling

The following simplifications have been adopted:

• incoming fluid at constant temperature T_{ing} and capacity;

• material and fluid contained in the channel initially at constant temperature on the whole domain T_{ini}, that is conditions of first heating;

• the implemented algorithm for analysing the discharge phase assumes as initial tempera-ture fields, both for fluid and solid, those calculated at the end of the charge phase;

• a fluid-dynamic analysis of the water flux within the channel is not conducted. The fluid system is treated via a 1D model whereas the solid domain is analysed via the FEM so that for each element the energy balance equation is solved (see e.g. [2]);

- concrete is modelled in a simplified manner as an homogeneous, continuous and isotropic material;

- the geometry is axis-symmetric.

Up to now all the procedures have been developed via CAST3M [16].

6.1. Development of a quasi-steady model

The first step is the implementation of a 1D model for the flux in the channel to be coupled with the FEM calculation. A quasi-steady procedure has been implemented in CAST3M on the basis of [13]. To validate the procedure, the results are compared to the reference ones. The physical channel model is shown in Figure 14.
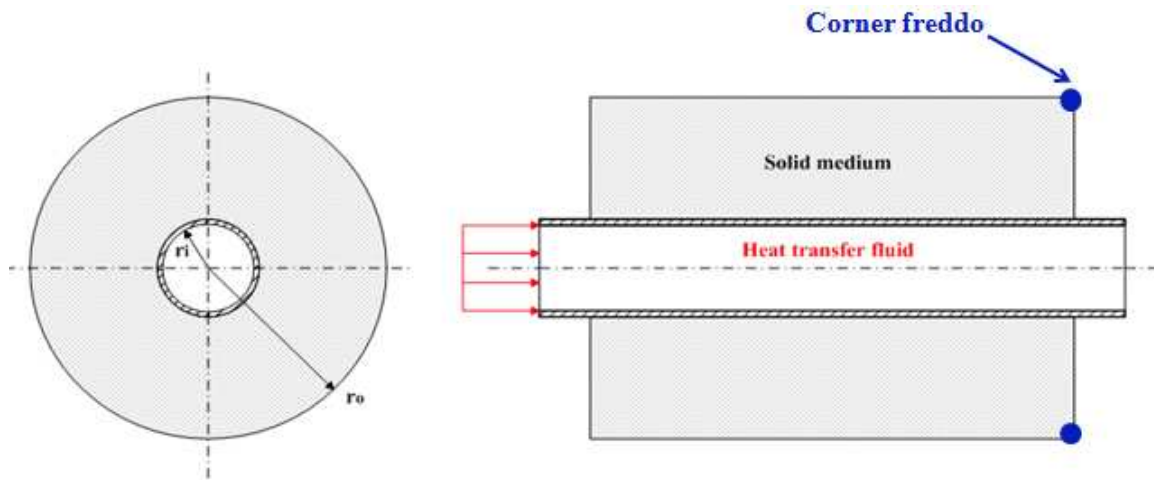

Figure 14. Channel geometry.

It consists in a concrete drilled cylinder with a fluid pumped through an internal pipe for heat exchange, with an adiabatic external surface ($r = r_0$). In order to solve the problem analytically, it is necessary to assume incoming velocity with a fully developed profile and negligible axial conduction in the solid medium.

The pipe has small thickness so that its thermal resistance is negligible; in this way the HTF is assumed to be in direct contact with the solid material.

The equation of the axial gradient for T_f is obtained by the energy balance on the channel element of length dz (Figure 15)

$$\rho c_p VA \cdot T_{f,in} - \rho c_p VA \cdot T_{f,out} - h \cdot 2\pi r_i dz \left(T_f - T_w\right) = \rho c_p A dz \cdot \frac{\partial T_f}{\partial t} \tag{18}$$

If neglecting the term of temporal variation for T,

$$\rho c_p VA \cdot T_{f,in} - \rho c_p VA \cdot T_{f,out} - h \cdot 2\pi r_i dz \left(T_f - T_w \right) = 0 \tag{19}$$
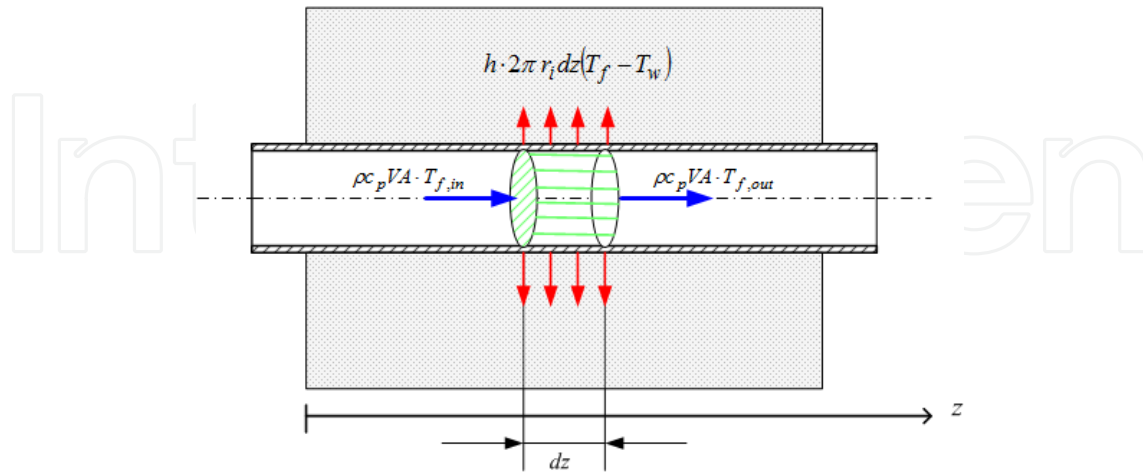

Figure 15. Energy balance for the fluid element.

where $A = \pi \, r_i^2$ is the crossed fluid section, V fluid velocity, $T_w = T_s(r_i)$ temperature of the channel wall.

By readjusting the terms

$$h \cdot 2\pi r_i \left(T_f - T_w \right) = \rho c_p VA \cdot \frac{\partial T_f}{\partial z} \tag{20}$$

So that, by isolating the term of spatial variation of T_f and introducing the crossed fluid section,

$$\frac{2h}{\rho c_p V r_i} \left(T_f - T_w \right) = \frac{\partial T_f}{\partial z} \tag{21}$$

Equation (21) is clearly non-linear for the presence of the unknown T_f on both sides; anyway, if for the term T_f within parenthesis a valid estimate can be given, the described relations reduce to linear differential equations of the first order which can be easily integrated so to give $T_f(z)$ at a specific time instant. In view of a step-by-step procedure in which a time discretization is performed, a valid estimate of T_f to be introduced in the l.h.s. is given by its value at the previous time-step.

To calculate the value of the known term, on the basis of the above discussed estimate of T_f, T_w values must be determined as well as the exchange coefficient h (via the Nusselt number) relative to the given conditions. As regards the former, it represents the output of the FEM calculation conducted on the domain corresponding to the zone occupied by concrete; for

the latter, for turbulent fluxes in a cylindrical channel, the local value of the dimensionless parameter (oil and water) is given by

$$Nu = \frac{Re \cdot Pr \cdot \left({c_f}/{2} \right)}{1.07 + 12.7 \cdot \left(Pr^{2/3} - 1 \right) \sqrt{{c_f}/{2}}} \tag{22}$$

where the friction coefficient is given by

$$\frac{c_f}{2} = \left(2.236 \ln Re - 4.639 \right)^{-2} \tag{23}$$

The range of validity of the above expression is $0.5 < Pr < 2000$, $10^4 < Re < 5 \times 10^6$.

By analysing the trend of the physical characteristic of liquid water and of the parameters used in the equation in which they appear (h and N_u), it can be noticed that the trends of N_u and h are weakly variable with temperature, as shown in Figure 16, so the choice of assuming constant values for these parameters and for water properties appears justified in the present model validation.
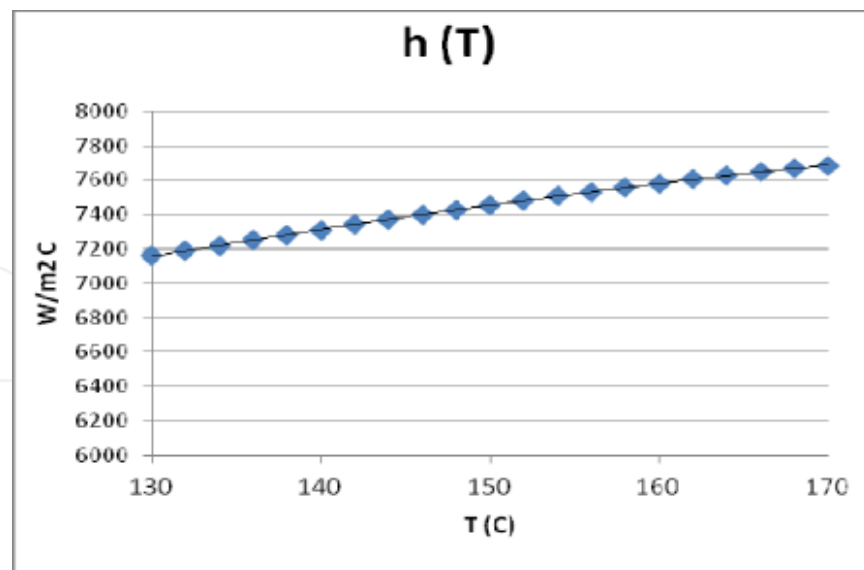

Figure 16. Variation of the thermal exchange coefficient of water with temperature.

After having implemented the numerical algorithm, the model characteristics relative to [13] and reported in Table 4 have been adopted.

r_i	r_o	L	T_{ing}	T_{ini}	ρ_S	c_{pS}	k_S	v_{H2O}
mm	mm	m	°C	°C	kg/m³	J/kg °C	W/m °C	m/s
13	65	2,6	90	25	2954	900	1	1

Table 4. Characteristics of the reference model.

Subsequently, a series of simulation runs have been launched by varying one of the listed parameters each time so to perform a sensitivity analysis; particularly thermal conductivity, external diameter and fluid velocity have been chosen. The analyses have allowed for obtaining time histories of temperature at the cold corner, i.e. at the concrete external circumference for the final section, representing the most hardly chargeable zone; the results have been then compared to the reference ones.

For sake of brevity, just the main observations are reported here:

- conductivity is evidently the parameter with a relevant influence on the storage charging mechanism considering that, by incrementing its value, temperature curves show higher slopes in correspondence of the considered zone; anyway, it is to be noticed that values around 5 W/m°C are physically unreachable with available concretes. Asymptotically, the results from the numerical code and those from the semi-analytical approach of [13] coincide;

- the system appears to be weakly sensitive to a variation in fluid velocity;

- the value of the internal radius has been maintained unaltered (that is the section crossed by the fluid and the characteristics of the convective exchange), so that the system capacity has been varied by changing the material thickness relative to the single pipe: the system appears to be strongly sensitive to a variation in the external radius.

6.2. Development of a non-steady model

The main weakness of the procedure described above is the difficulty linked to the number of iterations necessary to cover the entire channel length and to the integration of the various profiles; hence a new approach based on a non-steady model has been additionally developed.

A subdivision in axial cells of the channel has been realized so to follow the fluid along its path; the calculated temperature values are those related to the centre of the single cell.

The energy balance equation becomes (the capacity term is not neglected)

$$\rho c_p V A \cdot T_{f,i} - \rho c_p V A \cdot T_{f,u} - h \cdot 2\pi r_i dz \left(T_f - T_w\right) = \rho c_p A dz \cdot \frac{\partial T_f}{\partial t} \tag{24}$$

By discretizing the time variable

$$\rho c_p VA \cdot \left(T_{f,j-1} - T_{f,j}\right)\Big|_{t-1} - h \cdot 2\pi r_i \Delta z\left(T_{f,j} - T_{w,j}\right)\Big|_{t-1} = \rho c_p A\Delta z \cdot \frac{T_{f,j}\big|_t - T_{f,j}\big|_{t-1}}{\Delta t} \tag{25}$$

where j indicates the cell number, $T_{f,i} = T_{f,j-1}$ (T is evaluated at the centre of the cell and it is assumed, as incoming T in a cell, the value at the centre of the previous cell, Figure 17), t is the present time step and t-1 the previous one.
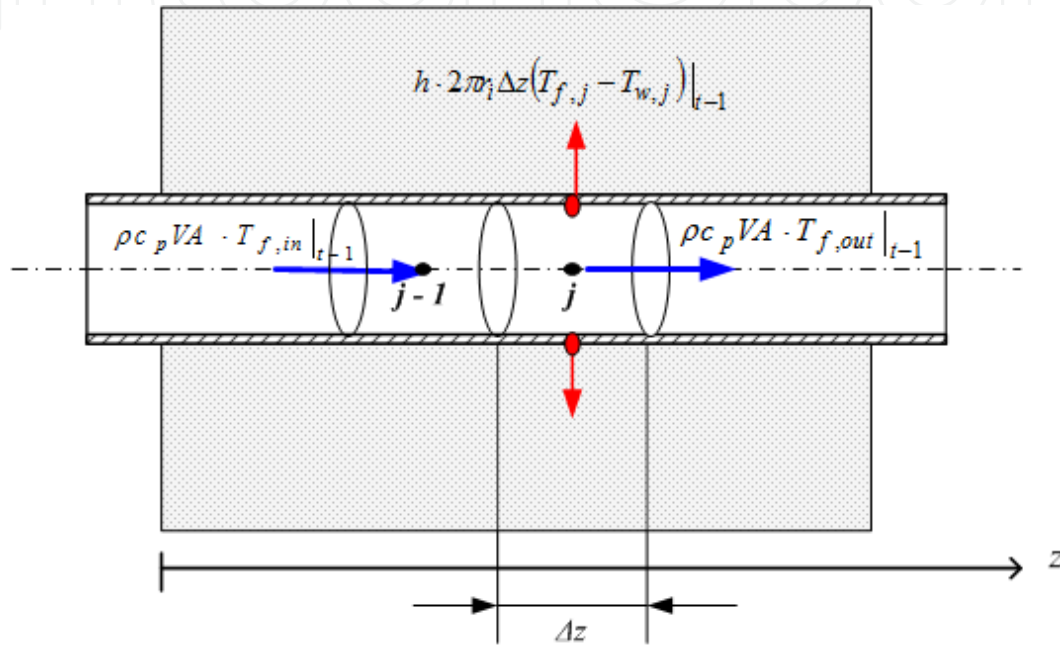

Figure 17. Definition of cells for the channel.

Hence T_f at the current t in the generic cell

$$T_{f,j}\big|_t = V\frac{\Delta t}{\Delta z} \cdot \left(T_{f,j-1} - T_{f,j}\right)\Big|_{t-1} - 2\pi \cdot r_i \Delta z \frac{h \cdot \Delta t}{\rho c_p A\Delta z}\left(T_{f,j} - T_{w,j}\right)\Big|_{t-1} + T_{f,j}\big|_{t-1} \tag{26}$$

The time history of T_f and the final temperature field in the channel can be obtained step-by-step. Differently to the quasi-steady approach, this one allows for visualizing the progression of the hot front linked to the fluid flow within the pipe. The sequence of Figure 18 shows what stated with reference to a 100 m channel.

The hot fluid (red) enters the channel by increasing the wall temperature (blue) only up to the distance to which the first front has arrived, then the instant at which such front reaches the final section becomes evident and subsequently the profiles move up together until reaching the final configuration.
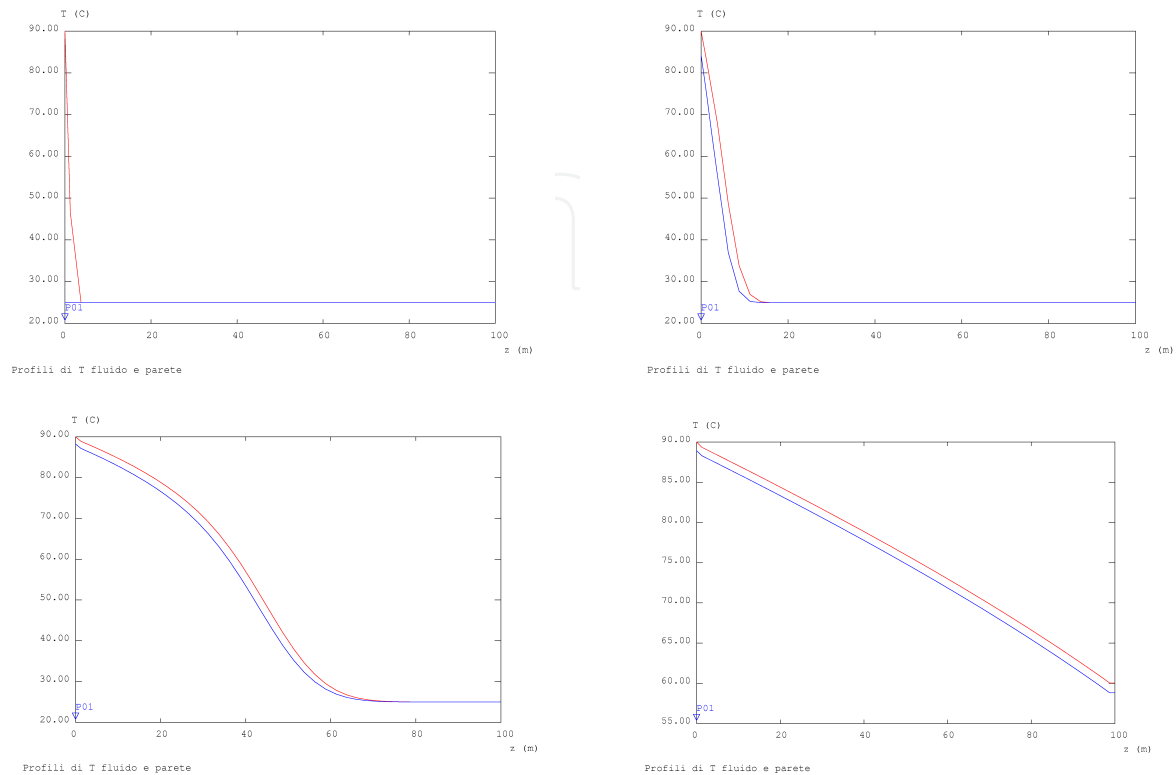
Figure 18. Fluid progression within the pipe.

Once again the approach has been validated against the results reported in [13] and the re-sults have also been compared with the ones of the quasi-steady analysis; it can be immedi-ately stated that for simulating a channel with limited length, the calculation times required by the present approach would be higher than those for the steady state (being possible to choose even large time-steps independently on the discretization of the grid). In fact a major restraint is now the time-step amplitude, being necessary that $\Delta t < \dfrac{\Delta z}{v_{liq}}$.

As an example, Figure 19 shows the time histories of temperature at the cold corner varying conductivity of the solid (1 and 3 W/m°C) and superimposing the present curve (black) with the ones from the quasi-steady analysis (blue) and from [13] (green): black and blue curves practically overlap, so that all validation issues (previously reported) apply even for the present approach. As an extension, for channels with length L < 10 m, the quasi-steady method allows for faster calculations -and susbstantially identical results- than the non-steady one. Hence it can be stated that the latter approach is efficient for analysing long channels, for which it is possible to assume Δz of the order of 1 ÷ 5 m and so even large Δts; under these assumptions even transients of about 1 h and channels of 100 ÷ 500 m can be solved in few minutes.
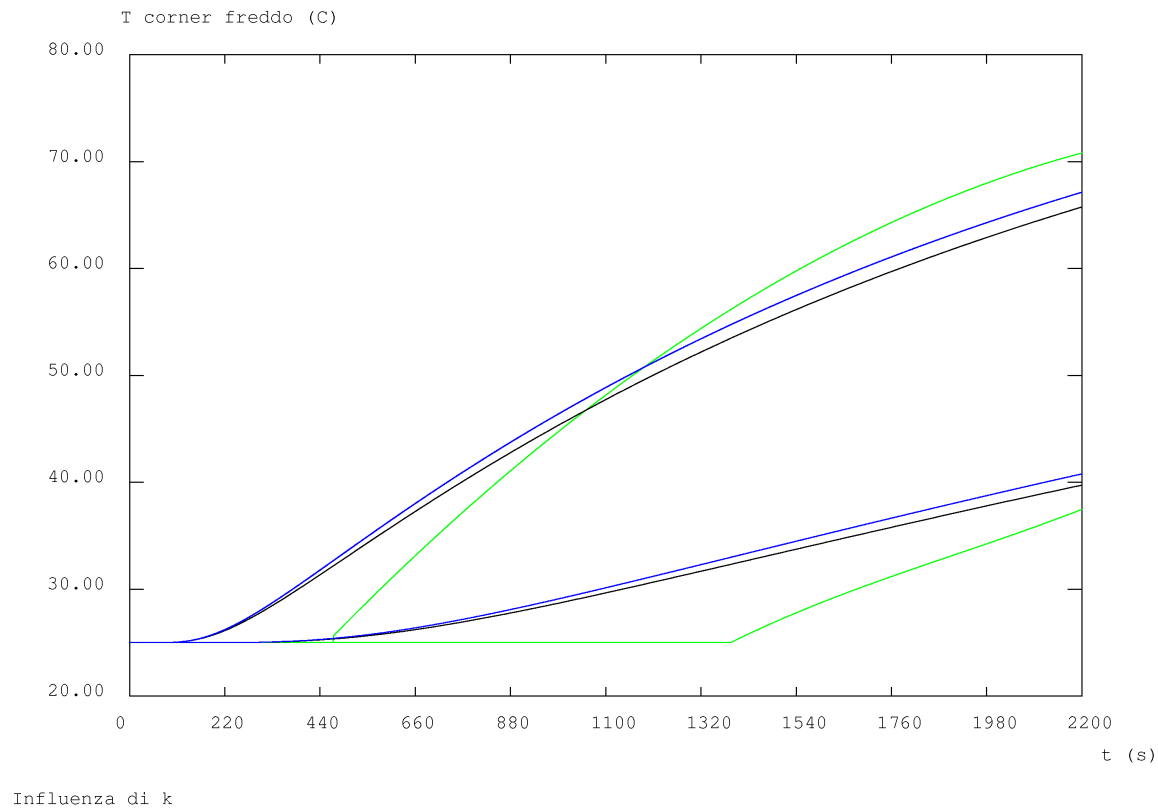
Figure 19. Comparison among quasi-steady (blue), analytical (green) and non-steady models.

By assuming the same input data as before, a 1 h transient analysis has been developed for a 400 m channel (500 m is a typical value for modules from DLR) and taking $\Delta z = 2,5$ m, $\Delta t = 2$ s; in Figure 20 the time histories of temperatures are depicted relatively to the external concrete circumference at the initial (yellow) and final (blue) section: the model follows the fluid in its own motion, so that temperature (initially fixed at $T_{ini} = 25$ °C for the whole material) starts increasing on the external corner of the initial section after a time equal to the one necessary for the radial diffusion of heat; at this time the hot front has not reached the cold one yet, which remains at the initial temperature. The blue curve starts rising after a time equal to the sum between the time of fluid transit in the channel and the one of radial diffusion of heat. Obviously, the temperature at the initial section is, at equal time, higher than the one at the exit section; additionally, considering the latter section, it comes out (the diagram has not been added for sake of brevity) that the time histories of temperature for the fluid, for the steel pipe surface and for the concrete in contact with the pipe substantially coincide (as predictable), so justifying the possibility of adopting models which neglect the steel pipe and assume direct contact between fluid and concrete.
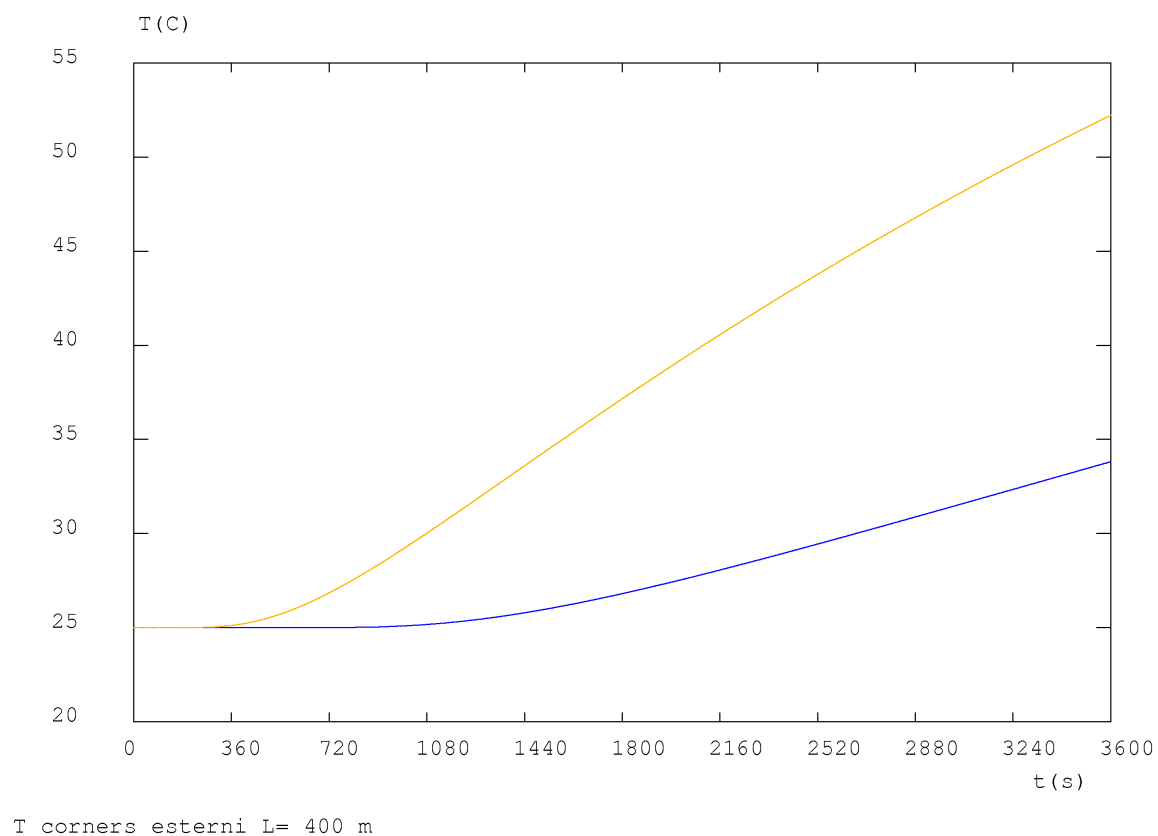
T corners esterni L= 400 m

Figure 20. Time history of temperature at extreme corners.

The non-steady model has been additionally used for simulating the discharge phase, not described here.

6.3. Energy issues

The FE code allows for even calculating the quantity of energy released by the fluid to concrete during the transient charge phase; with reference to the single channel of the examined configuration E_{cls}=279MJ. By multiplying this value by the number of chan- nels, the total stored energy in the module becomes E_{sto}=279MJ $\cdot$ 44=12200MJ, much lower to the 97200 MJ necessary to guarantee 6 hs storage. The situation is additionally worsened considering that the calculated energy value is overestimated with respect to the real one being referred to a charge cycle related to an initial field of uniform tem- perature within the solid equal to 80°C, so it is obtained by considering a ΔT higher than the effective one.

However, even if the obtained energy value is much lower than the one required dur- ing a preliminary plant design, it appears compatible with the formula for calculating the volume of material necessary to guarantee a fixed quantity of heat. In fact, for the considered geometry the volume results $V = N\pi\left(R_e^2 - r_i^2\right) \cdot L \approx 100m^3$ corresponding to about one tenth of the one which can be calculated on the basis of the nominal capaci-

ty of the plant system (see Table 3) [9]. The configuration has been consequently varied so to increase the storable heat quantity; the idea has been that to increase the number of channels in parallel, so it is necessary to decrease the single channel capacity to respect the plant restraint. The velocity of the flux has been so reduced from 1 m/s to 0.75 m/s leaving the geometry unaltered. By applying the simplified procedure, a channel length of 225 m is obtained for a total of 58 channels. Once checked that all the verifications conducted on the charge level and time are satisfied, a numerical simulation has been performed (final values for temperature on all sections have resulted to be the same as before). In this situation the energy released by the fluid to concrete for the single channel has been 209 MJ, so newly obtaining 12200 MJ.

Such a result was already predictable because generally true. In fact, if thermal losses towards the environment are neglected, in the charge phase $\Delta E_{cls} = \Delta E_{flu} = E_{f\_in} - E_{f\_out} \mid_{0}^{tc}$. By varying the capacity of the single channel, the total storage capacity, T_{in} and the trend of T_f on the final section (considering that the channel length is determined just imposing such a parameter) and the physical characteristics of the fluid remain unchanged, and so the last term of the expression above is unchanged. As a consequence, the storable solid energy is defined. Such a conclusion leads to formulate some observations on the material distribution within the storage module, that is on the convenience of having longer or shorter channels or, equivalently, if it is convenient to assume a high number of pipes in parallel.

The *comparison criterion* is that of the same material, i.e., as a first approximation, equal cost. Being the total capacity a parameter imposed by operational plant conditions, this must be the same whatever the number of modules in parallel; by having fixed the reference geometry for the transversal section, i.e. internal and external channel radius, and a charge time, two possibilities have been examined: 1) a channel with length L and fluid at velocity u; 2) two channels with length L/2 and fluid at velocity u/2 (the section is doubled).

The conclusion of this energy analysis of the charge phase has been that, at equal material and storable energy, a high number of channels in parallel with limited length is more convenient, i.e. with reduced velocities to reduce the charge losses along the pipes.

Such observations underline the potentialties of the developed procedure; in fact, even if it has not conducted to a satisfactory design of the storage module from the point of view of storable energy, it has anyway revealed:

- noticeable simplicity of application;

- reduced computational costs;

- reliability of produced results;

- capability of evidencing behavioural features of the component; particularly, it has been evidenced that the module storage capacity does not seem to represent a problem datum but a design consequence.

7. Conclusions

Guidelines for designing a concrete storage module and for its integration into a solar plant, respecting constraints linked both to an adequate solar field operation and to the production system based on ORC, have been described in this Chapter.

A series of simplified procedures have been developed to be used for a first module design and more sofisticated (even if more expensive) simulation techniques via the Finite Element Method have been checked and upgraded.

Once the ongoing experimental phase on a scaled storage prototype at the ENEA site of Casaccia has been concluded, the obtained data will be used for completing both the setup of the calculation instruments and the R&D activity dealing with the development of an appropriate concrete mixing, optimizing its chemical-physical and durability performances, and with the module integration within a CSP system.

Acknowledgments

Author details

Valentina A. Salomoni[1*], Carmelo E. Majorana[1], Giuseppe M. Giannuzzi[2], Rosa Di Maggio[3], Fabrizio Girardi[3], Domenico Mele[1] and Marco Lucentini[4]

*Address all correspondence to: valentina.salomoni@dicea.unipd.it

1 Department of Civil, Environmental and Architectural Engineering, University of Padua, Padua, Italy

2 ENEA – Agency for New Technologies, Energy and Environment, Thermodynamic Solar Project, CRE Casaccia, Rome, Italy

3 Department of Materials Engineering and Industrial Technologies, University of Trento, Trento, Italy

4 CIRPS, University of Rome "La Sapienza", Rome, Italy

References

[1] Giannuzzi G.M., Majorana C.E., Miliozzi A., Salomoni V.A., Nicolini D. Structural design criteria for steel components of parabolic-trough solar concentrators. Journal of Solar Energy Engineering 2007;129 382-390.

[2] Salomoni V.A., Majorana C.E., Giannuzzi G.M., Miliozzi A. Thermal-fluid flow within innovative heat storage concrete systems for solar power plants. International Journal of Numerical Methods for Heat and Fluid Flow 2008;18(7/8) 969-999.

[3] Laing D., Steinmann W.D., Tamme R. Solid Media Thermal Storage for Parabolic Trough Power Plants. Solar Energy 2006;80 1283–1289.

[4] Laing D., Lehmann D., Fiss M. Test Results of Concrete Thermal Energy Storage for Parabolic Trough Power Plants. Journal of Solar Energy Engineering 2009;131(4).

[5] Salomoni V.A., Majorana C.E., Giannuzzi G.M., Di Maggio R., Girardi F., Brunello P. Conceptual study of a thermal storage module for solar power plants with parabolic trough concentrators. In: Ubertini F, Viola E, de Miranda S, Castellazzi G (eds.) XX National Congress AIMETA, 12-15 Sept. 2011, Bologna, Italy. Conselice (Ra): Publi&Stampa; 2011.

[6] Di Maggio R., Ischia G., Bortolotti M., Rossi F., Molinari A. The microstructure and mechanical properties of Fe-Cu materials fabricated by pressure-less-shaping of nanocrystalline powders. Journal of Materials Science 2007;42 9284-9292.

[7] Laing D., Balh C., Bauer T., Lehmann D., Steinmann W.D. Thermal Energy Storage for Direct Steam Generation. Solar Energy 2011;85(4) 627–633.

[8] Tamme R., Laing D., Steinmann W.D. Advanced Thermal Energy Storage Technology for Parabolic Trough. ASME Journal of Solar Energy Engineering 2004;126 794-800.

[9] Santoro M. Study and analysis of thermal storage systems in cementitious materials for small size concentrated solar power plants. Master Thesis. ENEA-University of Rome "La Sapienza"; 2012.

[10] Sragovich D. Transient analysis for designing and predicting operational performance of a high temperature sensible thermal energy storage system. Solar Energy 1989;43(1) 7–16.

[11] Majorana C.E., Salomoni V, Schrefler B.A. Hygrothermal and mechanical model of concrete at high temperature. Materials and Structures 1998;31 378-386.

[12] Majorana C.E., Salomoni V.A., Mazzucco G., Khoury G.A. An approach for modeling concrete spalling in finite strains. Mathematics and Computers in Simulation 2010;80(8) 1694-1712.

[13] Bai F., Wang Z., Liye X. Numerical Simulation of Flow and Heat Transfer Process of Sol-id Media Thermal Energy Storage Unit. In Goswami D, Zhao Y (eds.) Solar Ener-

gy and Human Settlement: proceedings of ISES Solar World Congress 2007 (Vol. I-V). Springer; 2009;10 2711-15.

[14] Faghri A., Zhang Y. Transport Phenomena in Multiphase Systems. Burlington: Elsevier Inc.; 2006.

[15] Schumann T.E.W. Heat transfer: a liquid flowing trough a porous prism. Journal of the Franklin Institute 1929;208(3) 405–416.

[16] CAST3M Users' Manual, http://www-cast3m.cea.fr/.